BIOPHYSICS

Primary cilia as the nexus of biophysical and hedgehog signaling at the tendon enthesis

Fei Fang[1], Andrea G. Schwartz[2], Emily R. Moore[3], McKenzie E. Sup[1,4], Stavros Thomopoulos[1,4]*

The tendon enthesis is a fibrocartilaginous tissue critical for transfer of muscle forces to bone. Enthesis pathologies are common, and surgical repair of tendon to bone is plagued by high failure rates. At the root of these failures is a gap in knowledge of how the tendon enthesis is formed and maintained. We tested the hypothesis that the primary cilium is a hub for transducing biophysical and hedgehog (Hh) signals to regulate tendon enthesis formation and adaptation to loading. Primary cilia were necessary for enthesis development, and cilia assembly was coincident with Hh signaling and enthesis mineralization. Cilia responded inversely to loading; increased loading led to decreased cilia and decreased loading led to increased cilia. Enthesis responses to loading were dependent on Hh signaling through cilia. Results imply a role for tendon enthesis primary cilia as mechanical responders and Hh signal transducers, providing a therapeutic target for tendon enthesis pathologies.

INTRODUCTION

Tendon and its associated enthesis are essential components of the musculoskeletal system, linking muscle to bone to allow for coordinated muscle contraction, skeletal movement, and stability (*1*). This critical connection between muscle and bone, however, is prone to injury, accounting for a large number of musculoskeletal injuries in the United States every year (*1*–*3*). These injuries are often the result of overuse damage or underuse degeneration, leading to tendinopathy, enthesopathy, and eventually tissue rupture. Despite the prevalence of these injuries, no consensus treatments are available to prevent tendinopathy or enthesopathy or to recover a torn tissue to its native structure and full biomechanical functionality. There remains a critical gap in knowledge in our understanding of tendon enthesis responses to loading and the biological mechanisms that control these responses. The development of effective therapeutics is therefore hampered by our limited knowledge of tendon enthesis development biology, mechanobiology, and the endogenous mechanisms governing tendon pathogenesis and healing (*3*).

Both mechanical force and hedgehog (Hh) signaling are necessary for the development and maintenance of the tendon enthesis (*4*, *5*). Loading deprivation of mouse shoulders during postnatal development causes structural, compositional, and functional defects in the tendon enthesis, including reduced collagen fiber alignment, decreased mineral content, and impaired mechanical function (*6*). Conversely, application of moderate in vivo loading by treadmill running in both adult and aging mice shows beneficial effects, including increased gene expression related to tenogenesis, enhanced mechanical properties, and altered tendon composition (*7*). Hh signaling also drives enthesis fibrocartilage formation, mineralization, and healing. A unique population of Hh-responsive cells build the tendon enthesis at the postnatal stage (*5*, *8*, *9*). Ablation of these cells resulted in decreased fibrocartilage formation and collagen disorganization. Conditional deletion of Smoothened (Smo), a transmembrane protein necessary for Hh responsiveness, resulted in thinner fibrocartilage and decreased biomechanical function of the tendon enthesis (*5*, *8*, *9*). Enthesis cells with high Hh activation are also involved in enthesis healing, suggesting their importance for enhancing healing outcomes (*5*, *10*). Nonetheless, it has been a challenge to identify the cellular mechanism(s) controlling downstream cascades of mechanotransduction and the specific regulation of Hh signaling on tendon enthesis development and adaptation.

The primary cilium, an antenna-like nonmotile organelle that projects from the apical surface, is a critical component of intracellular biophysical and Hh signaling for many cells (*11*). Articular cartilage with disrupted primary cilia had increased thickness and reduced mechanical properties (*12*). Removal of primary cilia also markedly reduced loading-induced matrix deposition in chondrocytes (*13*). In bone, disruption of cilia formation in osteocytes resulted in a failure to trigger intracellular signaling cascades upon mechanical stimulation and a decrease in vivo bone formation (*14*). Furthermore, several components of the Hh signaling pathway, including Smo, are localized on or transduced inside the primary cilium itself, and Hh signaling activation and suppression are, in part, dependent on cilia (*11*). Mutation of ciliary proteins impairs Hh signaling, leading to ciliopathies such as cleft palate and polydactyly (*15*). These prior findings motivate our hypothesis that tendon enthesis formation and function are driven by cilia-dependent biophysical and Hh signaling. To test this hypothesis, we used tendon enthesis–specific mouse models and manipulated their physiological loading environments. We found that primary cilium incidence was temporally synchronized with Hh signaling during enthesis development. Enthesis cells responded to mechanical loading by inversely adjusting cilium incidence. Genetic disruption of cilia components led to defects in enthesis structure and mechanical properties. Furthermore, enthesis cell incidence was induced by the removal of Hh signaling and was coupled with diminished adaption to loading. Thus, our work revealed that primary cilia were at the nexus of mechanoresponsiveness and Hh signaling, directing tendon enthesis development and mediating its acclimatization to physiological loading.

RESULTS

Primary cilia are prevalent at the postnatal tendon enthesis

We previously demonstrated that Hh signaling is essential for tendon enthesis formation; furthermore, others have shown that primary cilia are critical for transduction of Hh signaling to musculoskeletal

[1]Department of Orthopedic Surgery, Columbia University, New York, NY, 10032, USA. [2]Department of Orthopedic Surgery, Washington University in St. Louis, St. Louis, MO, 63130, USA. [3]School of Dental Medicine, Harvard University, Cambridge, MA, 02138, USA. [4]Department of Biomedical Engineering, Columbia University, New York, NY 10027, USA.
*Corresponding author. Email: sat2@columbia.edu

cell nuclei (*5*, *15*). Therefore, we investigated tendon enthesis cell ciliogenesis during tendon enthesis development into maturity in a murine model. Antibodies against ciliary axoneme markers, including acetylated α-tubulin, *IFT88* (Intraflagellar transport protein 88) (ciliary axoneme markers), and/or the centrosome marker pericentrin, were used for immunostaining to detect primary cilia of supraspinatus tendon enthesis cells from different developmental stages (Fig. 1 and fig. S1). Cilium incidence (the number of ciliated cells normalized by the total cell number) of tendon enthesis cells increased markedly in the first 2 weeks postnatally, coincident with the pattern of Hh activation

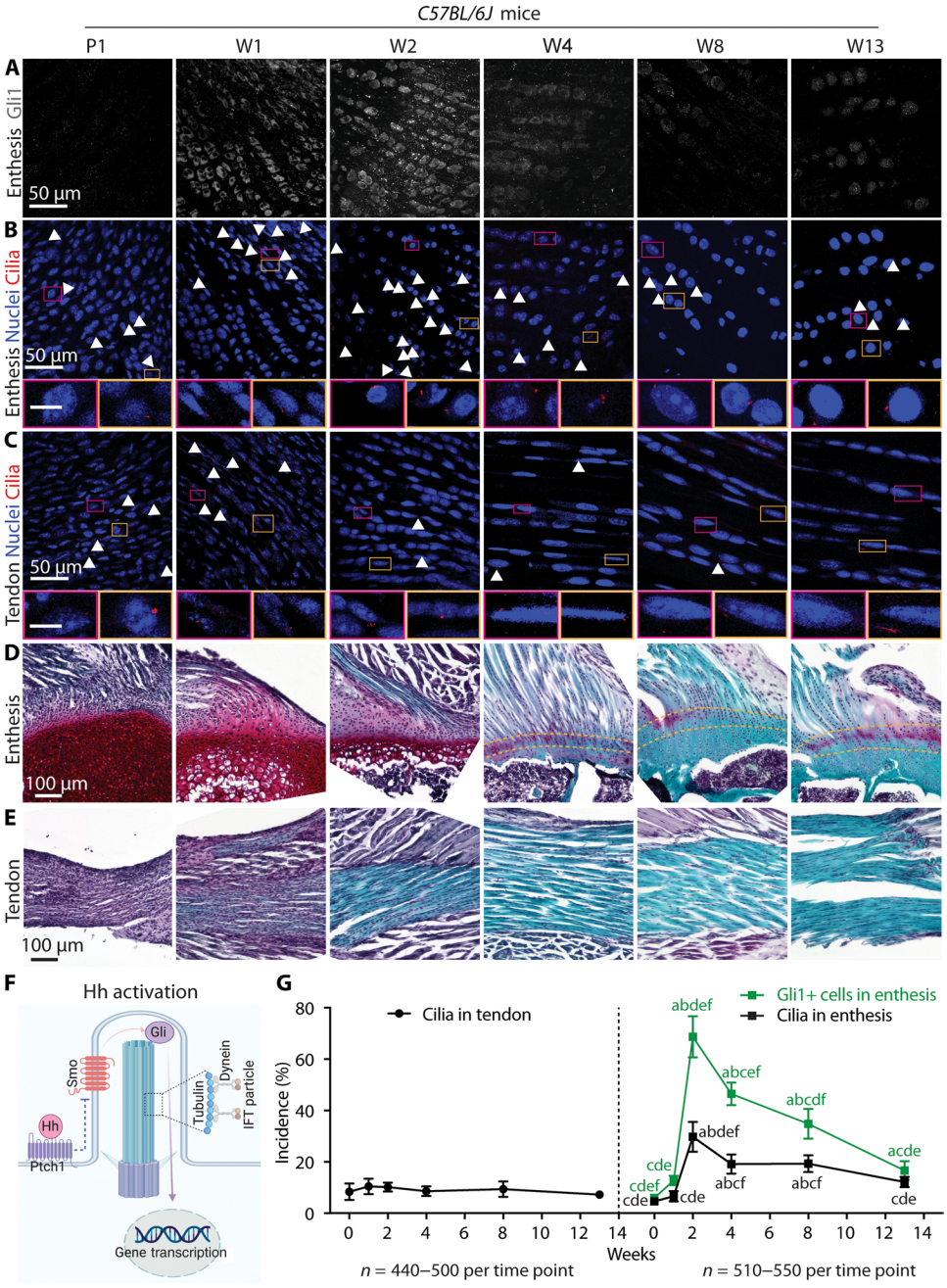

Fig. 1. Ciliogenesis of tendon enthesis cells during postnatal development coincides with Hh signaling and enthesis mineralization. (**A** to **C**) Immunofluorescence staining of Hh component Gli1 (gray) at the supraspinatus tendon enthesis (A) and primary cilia via acetylated tubulin (red, white arrowheads) at the enthesis (B) and midsubstance (C). Panels below (B) and (C) are magnified images corresponding to the colored rectangles. Arrowheads mark primary cilia; 4′,6-diamidino-2-phenylindole (DAPI) stains nuclei; P1, postnatal day 1; W1, postnatal week 1. Scale bars, 10 μm (panel insets). (**D** and **E**) Safranin O staining of the tendon enthesis and midsubstance at different developmental stages. Dashed lines mark the tendon enthesis. (**F**) Illustration of the transduction of Hh signaling inside the primary cilium. IFT, intraflagellar transport protein. (**G**) Quantification of the incidence of ciliated cells at the tendon and tendon enthesis as well as Gli1-positive (Gli1+) cells, normalized by the total cell number. Four to five mice were analyzed per time point; all data are represented as means ± SD; *n* represents the number of cells counted. a, $P < 0.05$ compared to W0; b, $P < 0.05$ compared to W1; c, $P < 0.05$ compared to W2; d, $P < 0.05$ compared to W4; e, $P < 0.05$ compared to W8; f, $P < 0.05$ compared to W13.

[i.e., glioma-associated oncogene (Gli1) expression] (Fig. 1, A, B, D, and G). In contrast, tendon midsubstance cells maintained a low level of ciliogenesis throughout postnatal development (Fig. 1, C, E, and G). The proportion of tendon entheses cells with cilia increased significantly between postnatal weeks 1 and 2 (W1 and W2), from 4.6 to 29.7%, and then decreased gradually to 12.1% by W13. Correspondingly, expression of Gli1 protein, the downstream effector of Hh signaling, changed in parallel with cell ciliogenesis during enthesis development (Fig. 1, A and G). Entheses cells had the highest activation of Gli1 and concurrent cilium incidence at W2 (Fig. 1G), coinciding with the onset of mineralization of the supraspinatus tendon enthesis (Fig. 1D) (*16*). These results imply that primary cilia contribute to Hh-driven and loading-regulated enthesis mineralization.

There is an inverse relationship between in vivo loading and primary cilium incidence

Motivated by the mechanosensory role of cilia in chondrocytes and osteocytes (*17*–*19*), we evaluated the connection between primary cilia incidence and tendon enthesis mechanoresponsiveness during postnatal development. Tamoxifen (TA)–inducible *GliCreER*^{T2};*Rosa26*^{mTmG} mice were used to track *Gli1*-lineage (*Gli1*-lin) cells. Mice were injected with TA at P14 (TA14) or P28 (TA28) and sacrificed at P56. Shoulders were paralyzed starting at birth using botulinum toxin A (BtxA) injection, a model that we previously established to unload the supraspinatus tendon enthesis and leads to defects in tendon enthesis formation (*6*). Compared to the entheses from contralateral control shoulders, unloading increased cilium incidence by 33% in TA14 mice and 66% in TA28 mice, respectively (Fig. 2, A to C). Similarly, unloading increased the *Gli1*-lin cell population by 48% in TA14 mice and 59% in TA28 mice (Fig. 2D). Unloading did not significantly change cilium incidence in the *Gli1*-lin cells in TA14 mice but resulted in a 31% decrease of cilium incidence in TA28 mice (Fig. 2E). However, cilium incidence of non–*Gli1*-lin cells was increased by 109 and 124% in TA14 and TA28 mice, respectively, after unloading (fig. S2). Unloading from birth through P56 led to significant up-regulation of genes related to ciliogenesis (e.g., *IFT88*, *IFT80*, and *Dync2li1*) and Hh signaling (e.g., *Ptch1*, *Gli1*, *Gli2*, and *Gli3*; Fig. 2E). These results demonstrate that biophysical forces drive ciliogenesis and activation of Hh signaling during enthesis development.

To determine mechanoresponsiveness of cilia in the adult enthesis, BtxA was used to unload tendon entheses, and treadmill running was used to overload tendon entheses (*7*). Consistent with the effects of unloading during development, 2 weeks of unloading led to increases of 166% in cilium incidence and 175% in Gli1-positive (Gli1+) cells (Fig. 3, A and C). Similarly, 4 weeks of unloading led to increases of 142% in cilium incidence and 128% in Gli1+ cells. In contrast to results during postnatal development, unloading of skeletally mature tendon entheses did not significantly change cilium incidence of Gli1+ cells, demonstrating that cilium assembly was not fully synchronized with Hh signaling in the adult tendon enthesis. In contrast to the effects of unloading, overloading led to a 48.7 and 56.8% decreases in cilium incidence after 2 and 4 weeks of treadmill running, respectively (Fig. 3, B and D). Running-induced overloading did not modify the population of Gli1+ cells nor did it change cilium incidence of Gli1+ cells. Overloading through 4 weeks of treadmill running led to down-regulation of genes related to ciliogenesis (i.e., *IFT88*, *Kif3A*, and *Dync2li1*) and Hh signaling (i.e., *Gli2*; Fig. 3E). In summary, unloading and overloading experiments in postnatal and adult animals demonstrate an inverse relationship between loading and cilium incidence/Hh activation.

Primary cilia are necessary for enthesis formation

The loading and unloading data demonstrate modulation of ciliogenesis at the tendon enthesis in response to in vivo loading. To extend our understanding of the role of primary cilia at the enthesis, we examined their necessity for enthesis formation. Tendon-specific (*Scx*-Cre) conditional deletion of *IFT88*, a ciliary gene, was achieved using *ScxCre*;*IFT88*$^{fl/fl}$ (cKO) mice (*20*). cKO mice had a 64% decrease in cilium incidence compared to their littermate controls (Fig. 4, A and E). Phenotype analysis from P10 to W13 demonstrated clear effects of cilia disruption on enthesis formation. The wild-type (WT) entheses had rounder and apparently larger cells compared to cKO, consistently from P10 to W13 (Fig. 4, B and C). This alteration in fibrocartilage cell phenotype was confirmed by changes in the expression of collagen X, a marker for hypertrophic chondrocytes; collagen X expression was significantly decreased by 67% in entheses from cKO mice compared to entheses from WT mice at 8 weeks (Fig. 4, C and F, and fig. S3D). Cortical and trabecular bone were not affected by *IFT88* knockout until W13 (Fig. 4G). At this time point, cKO mice had significantly deteriorated bone morphometry of the humeral head, with thinner cortical bone and less mineralized enthesis fibrocartilage (Fig. 4, C and G, and fig. S2, C and F). Furthermore, the tendon entheses from 13-week-old cKO mice had decreased structural properties (i.e., maximum force and stiffness) and increased material properties (i.e., stress and modulus; Fig. 4H), with drastically smaller cross-sectional areas in cKO tendon entheses (fig. S3A). *IFT88* knockout in *Scx*-expressing cells led to overall changes in mouse physiology. The growth of cKO mice was slower, with significantly lower body weights compared to WT controls (fig. S3A and B). Thirty percent of cKO mice died between W6 and W13, possibly due to polycystic kidney disease directly caused by deletion of IFT88. Loss of IFT88 in Scx-expressing cells resulted in altered mouse locomotion, e.g., swing speed and cadence (fig. S3A).

Ciliary Hh signaling mediates mature enthesis adaptation to in vivo loading

To examine the interaction between primary cilia, Hh signaling, and in vivo mechanical loading, we generated mice that harbored a tendon-specific loss of the Hh receptor *Smo* (*Smoothened*) and subjected them to unloading and overloading protocols (Fig. 5A). Deletion of *Smo* caused a 55.0% increase in tendon enthesis cells with primary cilia, indicating that cilia assembly was maintained or induced by Hh disruption (Fig. 5, B and D). Overloading and unloading also induced cilia disassembly and assembly, respectively, in the enthesis from *ScxCre*;*Smo*$^{fl/fl}$ cKO and WT mice, further demonstrating a mechanosensory role of cilia at the enthesis (Fig. 5D). Consistent with our previous study, loss of *Smo* in *Scx*-expressing cells led to a loss of enthesis fibrocartilage and decreased structural and material properties (Fig. 5, C and E to G, and fig. S4A). When considering enthesis mechanoresponsiveness, both overloading and unloading led to changes in enthesis mineralization (i.e., increased and decreased densities of cortical bone after overloading and unloading), bone morphometry, and mouse gait in WT mice (Fig. 5 and fig. S4). In contrast, Hh deletion mitigated many of these loading-induced changes to the tendon enthesis of WT mice: cross-sectional area in WT mice decreased after both overloading and unloading (Fig. 5E), stiffness and ultimate stress decreased after unloading, and ultimate

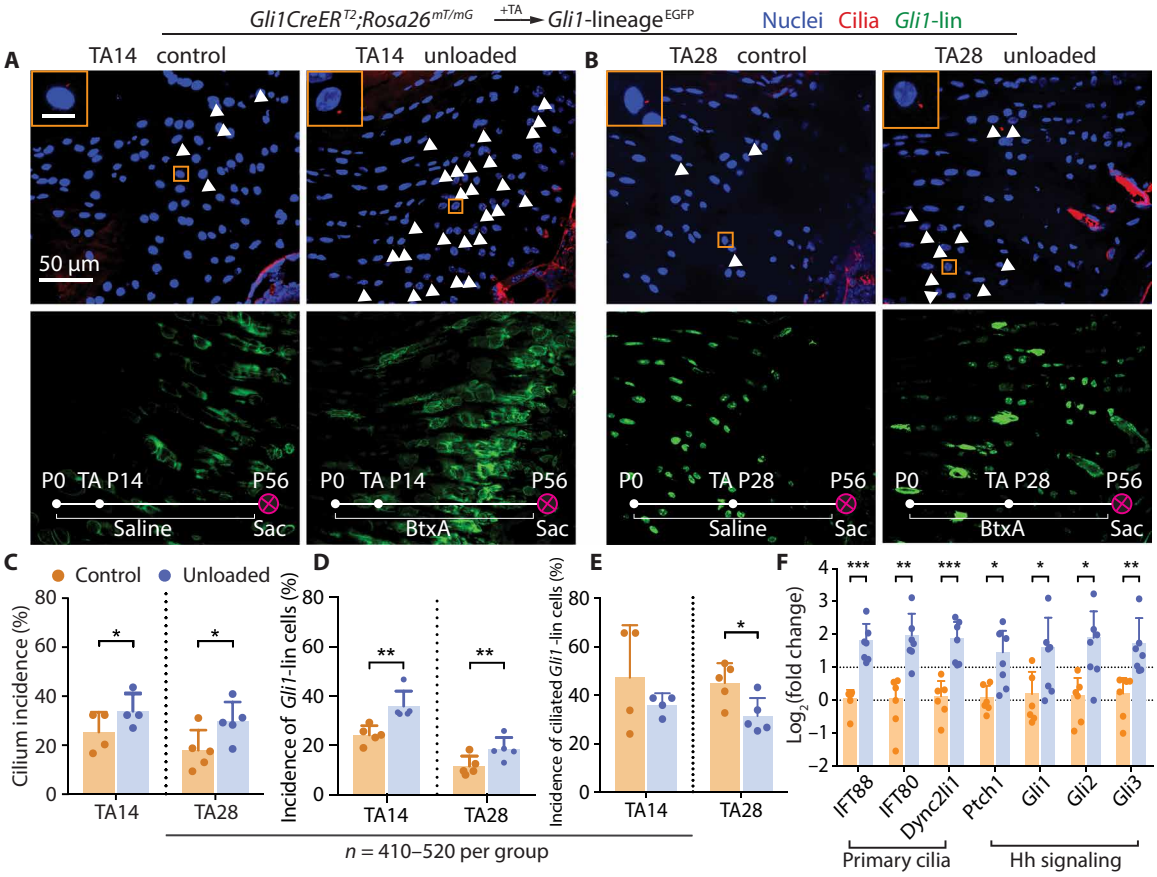

Fig. 2. Unloading during tendon enthesis development stimulates primary cilia assembly. (**A** and **B**) Immunofluorescence for primary cilia (red, white arrowheads) of the tendon enthesis from *GliCreER*^{T2};*Rosa26*$^{mT/mG}$ mice with TA injection and BtxA-induced paralysis (unloaded, right shoulder) or saline injection (control, left shoulder) at the time points indicated. Panels on the top left show magnified views of the orange rectangles. DAPI stains nuclei; P0, postnatal day 1; TA, tamoxifen injection; Sac, sacrifice; scale bar, 10 μm (inset). (**C**) Incidences of ciliated cells per all the cells at the tendon enthesis of (A) and (B) mice with TA injection at P14 and P28. *n* represents the number of cells counted. The error bars show SD of tissue samples from different animals. **P* < 0.05, ***P* < 0.01, ****P* < 0.001. (**D**) Incidences of *Gli1*-lin cells per all the cells at the tendon enthesis of (A) and (B) mice. (**E**) Incidences of ciliated *Gli1*-lin cells normalized by *Gli1*-lin cells at the tendon enthesis, showing the incidence of *Gli1*-lin cells that were ciliated. (**F**) Expression of genes related to primary cilia and Hh signaling from tendon entheses of 8-week-old C57BL/6J mice paralyzed since birth.

stress increased after overloading; none of these outcomes were affected by loading in *ScxCre*;*Smo*$^{fl/fl}$ cKO mice (Fig. 5F). When examining the morphometry of bone adjacent to the tendon enthesis, overloading increased and unloading decreased cortical bone densities (tissue mineral density) and trabecular bone densities (bone mineral density) in both genotypes (Fig. 5G). Similar results were seen in other bone morphometry outcomes (fig. S4B). At the whole animal level, both swing speed and cadence were increased by unloading for both genotypes (Fig. 5H and fig. S4C).

DISCUSSION

The current study demonstrated that tendon enthesis formation and function are driven by primary cilium-dependent biophysical and Hh signaling. We first identified that the primary cilium is critical for tendon enthesis mechanoresponsiveness. Ciliogenesis during enthesis development and maturity was inversely driven by physiological loading. In addition, cilium incidence at the tendon enthesis increased during enthesis mineralization and was synchronized with Hh signaling, supporting the concept of interplay between Hh signaling and cilia (*21*). This is consistent with previous reports that both primary cilia and Hh components change dynamically during muscle differentiation (*22*). Further evidence of this interplay was shown through deletion of Hh signaling, which caused abnormal ciliogenesis and diminished mechanoresponsiveness at the tendon enthesis. Most markedly, the deletion of primary cilia from the tendon enthesis caused significant structural and compositional defects to the enthesis. Therefore, primary cilia are key regulators of enthesis formation and maintenance, modulating their assembly in response to biophysical forces and their interaction with Hh signaling.

Consistent with the current in vivo results, an inverse relationship has been demonstrated previously between ciliogenesis and mechanical loading in vitro (*17*, *23*, *24*). Mechanical stimulation above a threshold leads to cilia shortening and disassembly, and removal of mechanical loading leads to cilia elongation and assembly (*24*–*26*). This response may be an effort of cilia to scale their sensitivity according to the loading signal. Cilium elongation or assembly increases the mechanosensitivity of the cilium or increases the number of mechanosensors on the ciliary membrane, respectively, which improves the cell's ability to sense mechanical cues from its environment

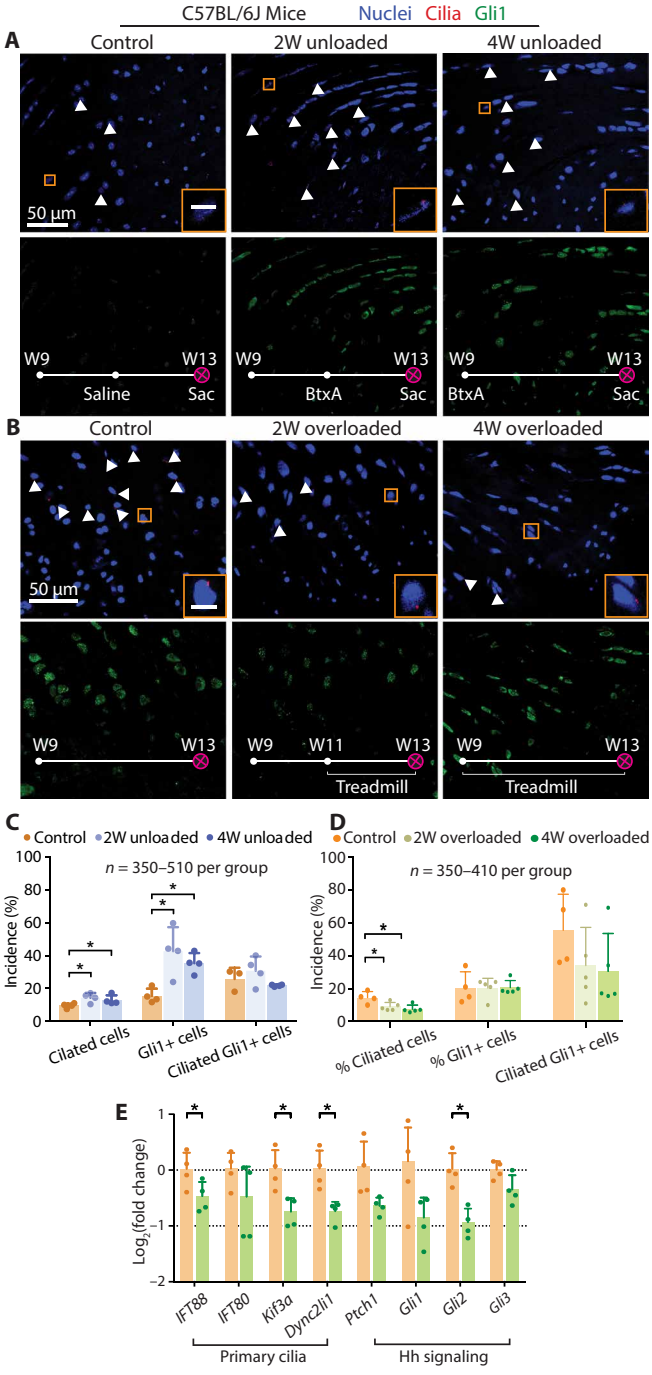

Fig. 3. Unloading and overloading of mature tendon entheses lead to cilia assembly and disassembly, respectively. (**A**) Immunofluorescence for primary cilia (red, white arrowheads) of the tendon entheses from 9-week-old C57BL/6J mice with BtxA (right, unloaded) or saline (left, control) injection at the time indicated on the images. 2W, 2 weeks; scale bar, 10 μm (inset). (**B**) Immunofluorescence for primary cilia of the tendon entheses from 9-week-old C57BL/6J mice after 4 weeks cage activity or 2 or 4 weeks treadmill running. (**C**) Quantification of the incidence of ciliated cells (per total cells), Gli1+ cells (per total cells), and ciliated Gli1+ cells (per Gli1+ cells) from (A). *$P < 0.05$. (**D**) Quantification of the incidence of ciliated cells (per total cells), Gli1+ cells (per total cells), and ciliated Gli1+ cells (per Gli1+ cells) from (B). (**E**) Expression of genes related with primary cilia and Hh signaling from tendon enthesis of 9-week-old C57BL/6J mice after 4-week cage activity or treadmill running.

(*15*). However, the exact mechanism(s) by which mechanical loading causes adjustment of cilium length or assembly of new cilia to form this feedback loop remains unknown. Ciliary disassembly is driven by the Aurora A–histone deacetylases 6 (HDAC6) cascade: Aurora A activates HDAC, a tubulin deacetylase, which promotes the depolymerization of acetylated α-tubulin as a ciliary scaffold, and then dismantles the ciliary organelle (*27*). In this context, the relationship between mechanical loading and Aurora A should be evaluated to further understand loading-mediated ciliogenesis (*28*). Additionally, mechanically induced osteogenesis may involve ciliary adenylyl cyclase 6 and cilia-dependent cyclic adenosine monophosphate, as an important early intracellular signal (*29*). Alternatively, the finding of primary cilia as enriched calcium compartments in tissues like the eye suggests that mechanosensing may be realized by calcium-permeable ion channels located at the ciliary membrane (*30*, *31*). However, there is still controversy about whether fluid flow causes ciliary calcium influx in bone and kidney cells (*23*, *30*, *32*, *33*) and biophysical signaling transduced by primary cilia may potentially be dependent on tissue-specific pathways. A better understanding of cilia-dependent mechanotransduction could facilitate development of small molecules to control ciliogenesis, e.g., by manipulating tubulin deacetylase and thereby tuning tissue sensitivity to biophysical forces.

Because of the constellation of many important signaling proteins along the ciliary membrane, mounting evidence reveals that primary cilia direct tissue developmental processes and control organ function, e.g., by regulating signaling pathways such as Hh (*15*). In musculoskeletal tissues, primary cilia disruption in osteogenic progenitors led to stunted limb growth and caused diminished load-induced bone formation (*20*). Loss of primary cilia in cartilage led to significantly increased thickness and reduced mechanical properties (*12*). Consistent with our cKO studies illustrating abnormal chondrocytes with reduced collagen X, mice without cilia in osteochondroprogenitors had aberrant proliferation and hypertrophic differentiation at the growth plate (*18*). Furthermore, cilia orientation in the growth plate was found to dictate cellular polarization and control cell stacking, although the mechanistic details were not defined (*34*). For the tendon enthesis, our study revealed the importance of primary cilia for enthesis formation and cilia-dependent mechanoresponsiveness in developing and mature tissues. Unfortunately, the mice lacking cilia in the tendon enthesis had kidney-related health issues, which precluded the implementation of unloading and overloading protocols.

The link between primary cilia and Hh signal transduction has been well characterized (*15*). Hh-related proteins are localized to ciliary membranes and trafficked from cilia to intracellular compartments, making them a necessary component of Hh signal transduction (*15*). Cilia deletion causes developmental defects such as shortened limb bones and other defects that mimic phenotypes observed in Hh-deficient mice (*15*). However, the potential for cross-talk between cilia and Hh signaling is understudied; it remains unclear whether Hh signaling contributes to cell ciliogenesis and/or mediates cilia-related mechanosensing. Counterintuitively, our observations showed that disrupted Hh signaling in tendon enthesis cells led to cilia maintenance/formation, contrary to a publication demonstrating that cilia deletion in myoblasts suppressed Hh signaling (*22*). In contrast, elongation of chondrocyte cilia after in vitro administration of lithium chloride inhibits Hh signaling, supporting a negative correlation between activation of Hh signaling and cilia

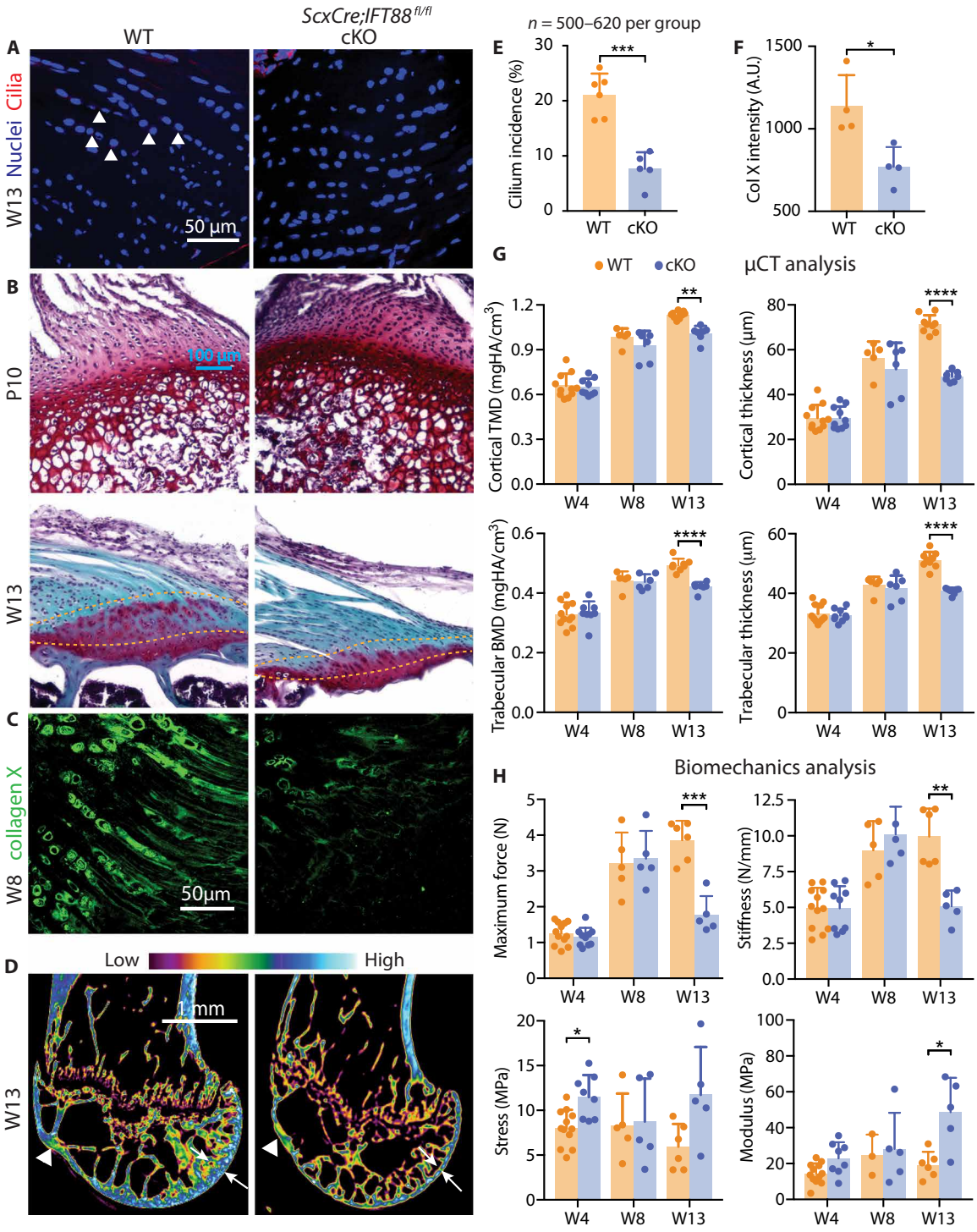

Fig. 4. Primary cilia are necessary for in tendon enthesis formation. (**A**) Immunofluorescence for primary cilia (red, white arrowheads) of tendon entheses from 13-week-old *ScxCre;IFT88*$^{fl/fl}$ (cKO) mice and their WT littermates. (**B**) Safranin O staining of the tendon entheses from WT and cKO mice at different time points. Dashed lines mark the tendon enthesis. (**C**) Immunostaining of collagen X at the tendon entheses from 8-week-old cKO and WT mice. (**D**) Microcomputed tomography (μCT) sections of humeral heads from 13-week-old WT and cKO mice. White arrowheads denote the supraspinatus tendon enthesis; white arrows denote bone thickness of humerus head. Color scale indicates low-to-high bone density. (**E**) Incidence of ciliated cells from (A). (**F**) Fluorescent intensity of collagen X (Col X) at the tendon enthesis from 8-week-old cKO and WT mice [e.g., as shown in (C)]. *$P < 0.05$, **$P < 0.01$, ***$P < 0.001$, ****$P < 0.0001$. A.U., arbitrary units. (**G**) Humeral head bone morphometry from 4-, 8-, and 13-week-old WT and cKO mice. TMD, tissue mineral density; BMD, bone mineral density. (**H**) Mechanical properties of the tendon enthesis from 4-, 8-, and 13-week-old WT and cKO mice.

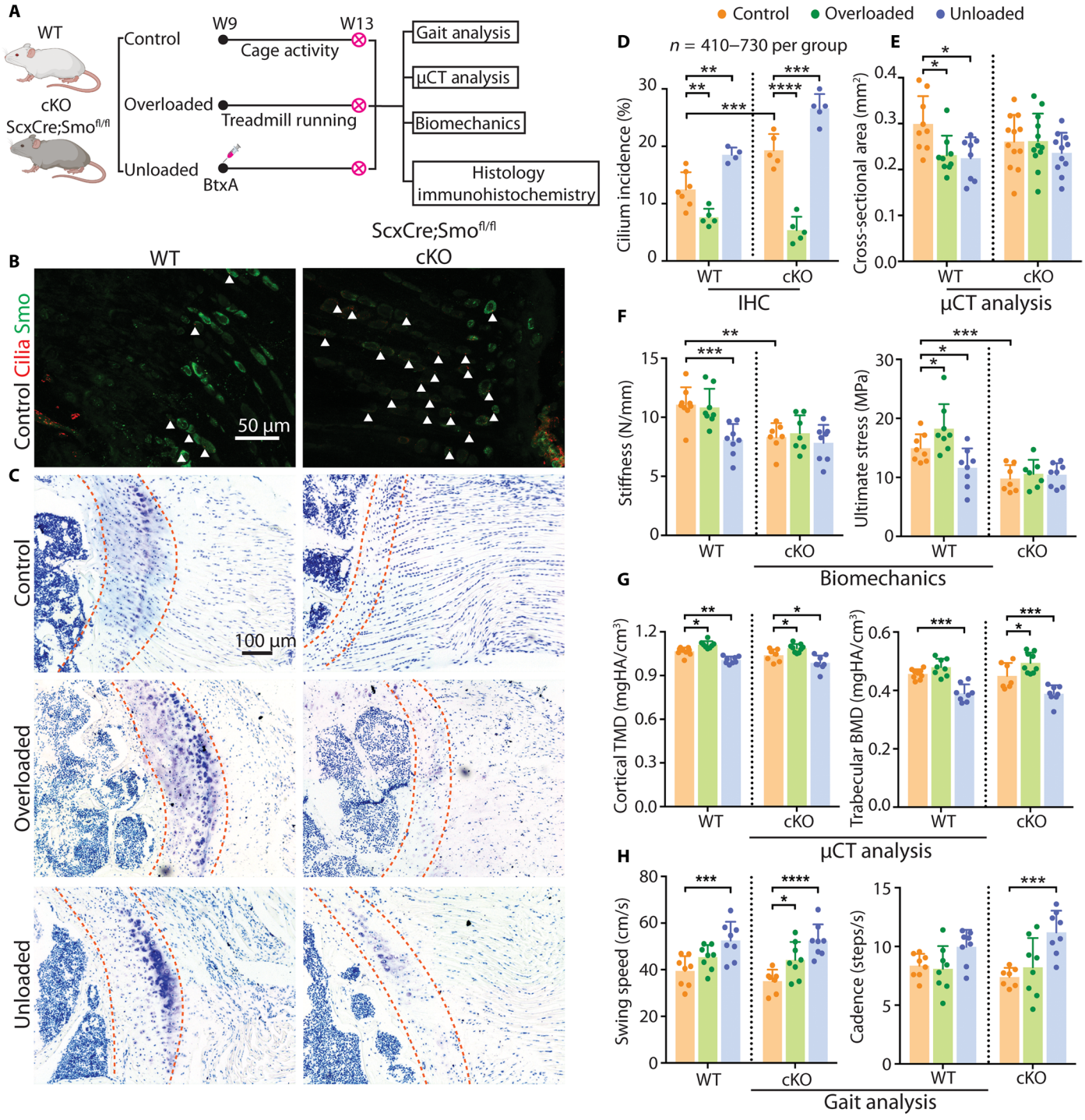

Fig. 5. Hh signaling is necessary for tendon enthesis responses to mechanical loading. (**A**) Experimental design. (**B**) Immunofluorescence of primary cilia (red, white arrowheads) and the Hh component Smo, (green) from 9-week-old *ScxCre;Smo*$^{fl/fl}$ mice (cKO) and their WT littermates. (**C**) Toluidine blue staining of the tendon entheses from 13-week-old WT and cKO mice after cage activity (control), BtxA-induced muscle paralysis (unloading), and treadmill running (overloading). Dashed lines mark the tendon enthesis. (**D** to **H**) Primary cilium incidence at the tendon enthesis (D) of WT and cKO mice subjected to cage activity (control), unloading, and overloading conditions; tendon cross-sectional area (E); tendon enthesis mechanical properties (F); bone quality of the humeral head (G); analysis of walking patterns (H). **P* < 0.05, ***P* < 0.01, ****P* < 0.001, *****P* < 0.0001. IHC, immunohistochemistry.

formation (*35*). Furthermore, since primary cilia during tumorigenesis have a dual role in activating and repressing Hh signaling depending on the oncogenic initiating event (*36*, *37*), regulation of cell ciliogenesis via Hh signaling might vary among different cell types and under varying loading conditions. Alternatively, increased cilia formation in *ScxCre*;*Smo*$^{fl/fl}$ cKO mice in the current study may have occurred as a compensatory mechanism in tendon enthesis cells that were not from the *Scx* lineage and hence retained their capacity for both Hh signaling and cilium assembly. Further evaluation of cellular cues coordinating the interplay between primary cilia and Hh signaling would be beneficial to decouple cilium mechanosensing and chemosensing roles. In the context examined here, the tendon enthesis with more ciliated fibroblasts caused by loss of Hh signaling had diminished sensitivity to their in vivo loading environment. Possibly with the increased but dysfunctional cilia, these mice lost their capacity to modify tendon enthesis biomechanics to adapt to their loading environment. Consistent with this hypothesis, recent reports indicate that application of hydrostatic compression or cyclic tension activates cilia-mediated Hh signaling, and disruption of cilia diminishes Hh activation by loading (*38*, *39*).

Primary cilia have been proposed as the nexus for coordinating responses to both mechanical loading and Hh signaling (*19*, *38*, *39*); however, the mechanisms underlying how primary cilia initiate intracellular signaling cascades induced by loading and coordinate Hh signaling remain unclear. In adult mice, we found that both cilia incidence and Hh signaling were activated by unloading. However, the experiment did not clarify the sequence of events, i.e., whether unloading induced ciliogenesis, which then prompted Hh signaling, or whether unloading induced Hh signaling, which then prompted ciliogenesis. In these adult mice, loading affected ciliation of cells at the enthesis; however, ciliation of Gli1+ cells (i.e., Hh-activated cells) was not significantly affected by loading. This implies a possible lack of synchronization of ciliogenesis and Hh signaling at the adult enthesis. In a different experiment, suppression of Hh signaling through deletion of *Smo* led to increased ciliogenesis, demonstrating cross-talk between the two. An alternative hypothesis is that unloading suppresses cell proliferation at the enthesis and mediates ciliogenesis, as ciliogenesis is tightly synchronized and regulated by the cell cycle (*40*). Intriguingly, we observed that unloading did not induce ciliation in Gli1+ cells and led to decreased ciliation in *Gli*-lin cells. In contrast, cells that were not from the *Gli* lineage responded to unloading with increased ciliogenesis. Therefore, a heterogeneous population of enthesis cells was ciliated during development of the tendon enthesis. These cells demonstrate spatial differentiation patterns, from tenocyte to chondrocyte to mineralized chondrocyte (*4*, *5*), which may be driven in part by ciliogenesis.

There were several limitations in the study. First, the musculoskeletal phenotype observed in *Scx*-driven IFT88 knockout mice could partially be attributed to off-target kidney-related health issues. Second, IFT88 has nonciliary functions such as regulation of cell mitosis (*41*) and therefore IFT88 knockout may have affected tendon enthesis cell proliferation. Second, the complexity of in vivo models makes it difficult to determine the exact mechanism(s) underlying cross-talk between primary cilia, Hh signaling, and biophysical forces. Better-targeted cilia knockout animal models and additional in vitro studies are needed to clarify the detailed mechanisms of the tendon enthesis formation mediated by primary cilia, and large animal models should be developed for future translational application of cilia-targeted therapies. Lastly, the imaging technique used to determine cilia presence did not have the resolution to accurately determine cilia length, which is an important indication of cell mechanoresponsiveness. Further studies are necessary to determine primary cilia orientation in tendon enthesis, and better imaging protocols should be established to capture cilia length with high resolution and speed.

The primary cilium plays a central role in differentiation and mechanosensing of many musculoskeletal tissues, and the current study offers new insights on the necessity of cilia for maintaining tendon enthesis health. These results have broader implications for musculoskeletal tissue repair and regeneration. Targeting cilia to treat musculoskeletal conditions has been demonstrated in muscle: Diminished cilia assembly led to activated myoblast proliferation and inhibited differentiation (*22*), and genetic deletion of cilia in muscle fibro-adipogenic progenitors suppressed intramuscular adipogenesis and enlarged myofiber size in a Hh-dependent manner (*42*, *43*). Accordingly, we illustrated the function of primary cilia as a hub of mechanical and Hh signal transduction using in vivo tendon-specific animal models. Because excessive or insufficient physical loading is a primary driver of tendon formation and enthesis pathologies, primary cilia are prime targets whose mechanosensitivity could potentially be tuned to prevent progression of these pathologies (*44*, *45*). For example, a long-standing hypothesis is that enthesitis is triggered and exacerbated by mechanical loading (*1*). In this context, desensitizing enthesis cells by suppressing cilia could prevent or treat that pathology. Furthermore, targeting primary cilia with small-molecule inhibitors or agonists may lead to replacement or optimization of mechanically based rehabilitation strategies for treating tendon disorders. Our studies provide a strong basic science rationale for cilia as a central regulator of mechanoresponsiveness and Hh signaling in the tendon enthesis, thereby providing an attractive therapeutic target for tendon and enthesis pathologies (*46*).

MATERIALS AND METHODS

Mouse strains

C57BL/6J mice, *Gli1CreER*^{T2} mice, *Rosa26*$^{mT/mG}$ mice, and *Smo*$^{fl/fl}$ mice were purchased from the Jackson laboratory. *ScxCre* mice, which drive a Cre-recombinase sequence by an *Scx* promoter, were provided by R. Schweitzer (*47*). Animals were housed and bred under standard Institutional Animal Care and Use Committee guidelines. The Columbia University Institutional Animal Care and Use Committee approved all experiments. To study cilia formation, postnatal mice from breeding pairs of C57BL/6J mice were euthanized at P1, W1, W2, W4, W8, and W13. To examine cross-talk among primary cilia, mechanical loading, and Hh signaling, reporter mice were generated by crossing tendon enthesis–specific *Gli1-CreER*^{T2} mice with *Rosa26*$^{mT/mG}$ mice. TA was injected at P14 and P28 to identify *Gli1*-lin cells from those time points. Since IFT88 is a core intraflagellar transport protein mediating ciliogenesis, tendon-specific cilia knockout mice were generated by crossing *ScxCre* mice with *IFT88*$^{fl/fl}$ mice. To evaluate mechanical responses of the tendon enthesis without Hh signaling, *ScxCre* mice were crossed with *Smo*$^{fl/fl}$ mice.

Overloading and unloading models

Overloading was achieved by running 9-week-old mice on a treadmill. After the training at a speed of 25 cm/s for 10 min for five

consecutive weekdays, mice were subjected to treadmill running for 4 weeks, with an initial rate of 20 cm/s for 10 min and then 28 cm/s for 40 min each weekday (*2*). Age-matched cage activity mice were used as controls. Unloading was achieved in 9-week-old mice by injecting BtxA (0.02 U/g; Allergan) into the supraspinatus muscles of the right limb (*4*, *6*). The contralateral limbs were injected with the same amount of saline and served as controls. Gli1+ cells at the adult tendon enthesis after overloading and unloading were identified using immunohistochemistry. For postnatal mice, 0.2 U of BtxA in saline was delivered to mouse shoulder muscles twice per week from birth until 4 weeks and then once per week through sacrifice at P56. Similarly, the contralateral limbs, injected with saline, served as controls. To identify *Gli1*-lin cells at P14 and P28, TA was dissolved in corn oil and injected intraperitoneally at P14 or P28. Similarly, *Gli1*-lin cells of tendon enthesis from postnatal mice after unloading were identified using immunofluorescence.

Gait analysis

Eight- and 13-week-old mice were subjected to gait functional evaluation (Noldus, CatWalk XT), and spatiotemporal data of footprints were processed for forelimbs. Briefly, a high-speed color camera captured mouse footprints with accurate spatial and temporal resolution, while mice voluntarily traversed a glass walkway. To identify changes of footfalls and locomotion, the catwalk XT software was used to calculate numerous parameters from three complete runs with speed variance less than 20%. Cadence was calculated as the number of steps per second. Swing speed was defined as the stride length of the forelimb paws normalized by swing time (*48*).

Gene expression using real-time RT-PCR

The supraspinatus tendon and enthesis were harvested, frozen in liquid nitrogen, and pulverized in a ball mill homogenizer (Mikro-Dismembrator U, Sartorius). Total RNA was extracted by TRIzol reagent and Invitrogen PureLink RNA Mini kit, as described in our previous study (*2*). The High-Capacity cDNA Reverse Transcription Kit (Invitrogen) was used to reverse transcribe RNA into cDNA. The relative abundance of cilium- and Hh signaling–related genes was evaluated by SYBR Green-based quantitative reverse transcription polymerase chain reaction (RT-PCR) on an Applied Biosystems QuantStudio 6 flex system. The sequences of RT-PCR primers used here are listed in table S1. Glyceraldehyde 3-phosphate dehydrogenase serves as housekeeping gene, and the relative mRNA expression level for each target gene was determined as $2^{-\Delta\Delta Ct}$.

Histology and immunohistochemistry

Mouse supraspinatus tendon-bone samples were dissected, fixed in 4% paraformaldehyde for 16 hours, and decalcified in 0.5 M EDTA for 2 weeks. Following embedding in optimal cutting temperature compound, 6-μm-thick sections were cryosectioned and stained with toluidine blue or safranin O according to standard protocols. For immunostaining, 10-μm-thick sections were predigested in hyaluronidase (2 mg/ml) for 1 hour and washed in 0.5% Triton X-100/phosphate-buffered saline (PBS). After washing, blocking was conducted with 15% goat serum/PBS, followed by incubation of sections at 4°C overnight with primary antibody and appropriate secondary antibody (table S2) for 1 hour at room temperature. Slides were mounted with mounting media for imaging on a Nikon Ti Eclipse inverted microscope with a 60× oil objective for visualization of primary cilia. Cilia quantification was conducted using ImageJ software (National Institutes of Health). The incidences of ciliated cells and Gli1+ cells (normalized by the total cell number, at least 100 cells for each sample) were determined from histologic sections. The incidence of *Gli1*-lin cells with cilia was determined as the number of *Gli1*-lin cells with cilia divided by the number of *Gli1*-lin cells. The images displayed are maximal projection of image stacks.

Microcomputed tomography

Bone morphometry analysis was performed on supraspinatus tendon-humeral bone samples. Samples were scanned at an energy of 55 kilovolt peaks, an intensity of 145 μA, and a standard resolution of 5 μm [microcomputed tomography (μCT), Bruker Skyscan 1272]. After image construction, a segmentation algorithm was conducted to separate cortical and trabecular bone of the humeral head proximal to the growth plate (CTAn, Bruker).

Tendon-bone biomechanics

Tendon-bone samples from μCT were prepared for tensile biomechanical testing. Humerus bone was inserted into a customized three-dimensional printed fixture, and tendon was clamped in thin film grips (*49*). Sample and grip assemblies were mounted on a testing frame with the incubation of PBS at 39°C (44.5 N load cell; ElectroPuls 1000, Instron Corp.). The samples were preconditioned between 0.05 and 0.2 N for 5 cycles, held for 300 s, and extended to failure with 0.2%/s. The tendon cross-sectional area was determined from constructed μCT images. Tendon structural and material parameters were calculated from recorded load-deformation data.

Statistical analysis

All data are presented as means ± SD of 5 to 12 biological replicates for gait analysis, biomechanics, and microcomputed tomography, 4 to 6 biological replicates for histology/immunohistochemistry, and 4 to 7 biological replicates for gene expression (table S3). For every experiment, both male and female mice from at least two independent litters were used. All data analyses were performed by a blinded analyzer. GraphPad Prism 7 was used to perform paired *t* tests, unpaired *t* tests (where appropriate), and analysis of variance (ANOVA); the mouse genotype and loading groups were considered as independent variables. Specifically, cilium incidence and gene expression of unloaded *GLI1CreER*^{T2};*Rosa26*$^{mT/mG}$ mice were compared with paired *t* tests; cilia incidence and gene expression of C57BL/6J mice were compared by one-way ANOVA or paired *t* tests; comparison of mechanical and structural properties of *ScxCre*;*IFT88*$^{fl/fl}$ mice were conducted by two-way ANOVA with Boferroni multiple comparisons test; mechanical and structural properties of *ScxCre*;*Smo*$^{fl/fl}$ mice under different loading conditions were compared by two-way ANOVA with Dunnett's multiple comparisons test. $P < 0.05$ was considered significant.

SUPPLEMENTARY MATERIALS

Supplementary material for this article is available at http://advances.sciencemag.org/cgi/content/full/6/44/eabc1799/DC1

View/request a protocol for this paper from *Bio-protocol*.

REFERENCES AND NOTES

1. G. Schett, R. J. Lories, M.-A. D'Agostino, D. Elewaut, B. Kirkham, E. R. Soriano, D. McGonagle, Enthesitis: From pathophysiology to treatment. *Nat. Rev. Rheumatol.* **13**, 731–741 (2017).

2. A. C. Abraham, S. A. Shah, M. Golman, L. Song, X. Li, I. Kurtaliaj, M. Akbar, N. L. Millar, Y. Abu-Amer, L. M. Galatz, S. Thomopoulos, Targeting the NF-κB signaling pathway in chronic tendon disease. *Sci. Transl. Med.* **11**, eaav4319 (2019).
3. G. Nourissat, F. Berenbaum, D. Duprez, Tendon injury: From biology to tendon repair. *Nat. Rev. Rheumatol.* **11**, 223–233 (2015).
4. A. G. Schwartz, L. M. Galatz, S. Thomopoulos, Enthesis regeneration: A role for Gli1+ progenitor cells. *Development* **144**, 1159–1164 (2017).
5. A. G. Schwartz, F. Long, S. Thomopoulos, Enthesis fibrocartilage cells originate from a population of Hedgehog-responsive cells modulated by the loading environment. *Development* **142**, 196–206 (2014).
6. A. G. Schwartz, J. H. Lipner, J. D. Pasteris, G. M. Genin, S. Thomopoulos, Muscle loading is necessary for the formation of a functional tendon enthesis. *Bone* **55**, 44–51 (2013).
7. B. P. Thampatty, J. H.-C. Wang, Mechanobiology of young and aging tendons: In vivo studies with treadmill running. *J. Orthop. Res.* **36**, 557–565 (2018).
8. N. A. Dyment, A. P. Breidenbach, A. G. Schwartz, R. P. Russel, L. Aschbacher-Smith, H. Liu, R. Hagiwara, R. Jiang, S. Thomopoulos, D. L. Butler, D. W. Rowe, Gdf5 progenitors give rise to fibrocartilage cells that mineralize via hedgehog signaling to form the zonal enthesis. *Dev. Biol.* **405**, 96–107 (2015).
9. A. P. Breidenbach, L. Aschbacher-Smith, Y. Lu, N. A. Dyment, C.-F. Liu, H. Liu, C. Wylie, M. Rao, J. T. Shearn, D. W. Rowe, K. E. Kadler, R. Jiang, D. L. Butler, Ablating hedgehog signaling in tenocytes during development impairs biomechanics and matrix organization of the adult murine patellar tendon enthesis. *J. Orthop. Res.* **33**, 1142–1151 (2015).
10. C.-F. Liu, A. Breidenbach, L. Aschbacher-Smith, D. Butler, C. Wylie, A role for hedgehog signaling in the differentiation of the insertion site of the patellar tendon in the mouse. *PLOS ONE* **8**, e65411 (2013).
11. Z. Anvarian, K. Mykytyn, S. Mukhopadhyay, L. B. Pedersen, S. T. Christensen, Cellular signalling by primary cilia in development, organ function and disease. *Nat. Rev. Nephrol.* **15**, 199–219 (2019).
12. J. Irianto, G. Ramaswamy, R. Serra, M. M. Knight, Depletion of chondrocyte primary cilia reduces the compressive modulus of articular cartilage. *J. Biomech.* **47**, 579–582 (2014).
13. A. K. T. Wann, N. Zuo, C. J. Haycraft, C. G. Jensen, C. A. Poole, S. R. McGlashan, M. M. Knight, Primary cilia mediate mechanotransduction through control of ATP-induced Ca^{2+} signaling in compressed chondrocytes. *FASEB J.* **26**, 1663–1671 (2011).
14. S. Temiyasathit, W. J. Tang, P. Leucht, C. T. Anderson, S. D. Monica, A. B. Castillo, J. A. Helms, T. Stearns, C. R. Jacobs, Mechanosensing by the primary cilium: Deletion of Kif3A reduces bone formation due to loading. *PLOS ONE* **7**, e33368 (2012).
15. F. Bangs, K. V. Anderson, Primary cilia and mammalian hedgehog signaling. *Cold Spring Harb. Perspect. Biol.* **9**, a028175 (2017).
16. A. G. Schwartz, J. D. Pasteris, G. M. Genin, T. L. Daulton, S. Thomopoulos, Mineral distributions at the developing tendon enthesis. *PLOS ONE* **7**, e48630 (2012).
17. S. Fu, C. L. Thompson, A. Ali, W. Wang, J. P. Chapple, H. M. Mitchison, P. L. Beles, A. K. T. Wann, M. M. Knight, Mechanical loading inhibits cartilage inflammatory signalling via an HDAC6 and IFT-dependent mechanism regulating primary cilia elongation. *Osteoarthr. Cartil.* **27**, 1064–1074 (2019).
18. E. R. Moore, Y. Yang, C. R. Jacobs, Primary cilia are necessary for Prx1-expressing cells to contribute to postnatal skeletogenesis. *J. Cell Sci.* **131**, jcs217828 (2018).
19. R. Ruhlen, K. Marberry, The chondrocyte primary cilium. *Osteoarthr. Cartil.* **22**, 1071–1076 (2014).
20. E. R. Moore, J. C. Chen, C. R. Jacobs, Prx1-expressing progenitor primary cilia mediate bone formation in response to mechanical loading in mice. *Stem Cells Int.* **2019**, 3094154 (2019).
21. F. K. Bangs, N. Schrode, A.-K. Hadjantonakis, K. V. Anderson, Lineage specificity of primary cilia in the mouse embryo. *Nat. Cell Biol.* **17**, 113–122 (2015).
22. W. Fu, P. Asp, B. Canter, B. D. Dynlacht, Primary cilia control hedgehog signaling during muscle differentiation and are deregulated in rhabdomyosarcoma. *Pro. Natl. Acad. Sci. U.S.A.* **111**, 9151–9156 (2014).
23. A. M. D. Malone, C. T. Anderson, P. Tummala, R. Y. Kwon, T. R. Johnston, T. Stearns, C. R. Jacobs, Primary cilia mediate mechanosensing in bone cells by a calcium-independent mechanism. *Pro. Natl. Acad. Sci. U.S.A.* **104**, 13325–13330 (2007).
24. D. T. Rowson, J. C. Shelton, H. R. Screen, M. M. Knight, Mechanical loading induces primary cilia disassembly in tendon cells via TGFβ and HDAC6. *Sci. Rep.* **8**, 11107 (2018).
25. K. Gardner, S. P. Arnoczky, M. Lavagnino, Effect of in vitro stress-deprivation and cyclic loading on the length of tendon cell cilia in situ. *J. Orthop. Res.* **29**, 582–587 (2011).
26. S. R. McGlashan, M. M. Knight, T. T. Chowdhury, P. Joshi, C. G. Jensen, S. Kennedy, C. A. Poole, Mechanical loading modulates chondrocyte primary cilia incidence and length. *Cell Biol. Int.* **34**, 441–446 (2010).
27. E. N. Pugacheva, S. A. Jablonski, T. R. Hartman, E. P. Henske, E. A. Golemis, HEF1-dependent Aurora A activation induces disassembly of the primary cilium. *Cell* **129**, 1351–1363 (2007).
28. M. Spasic, C. R. Jacobs, Lengthening primary cilia enhances cellular mechanosensitivity. *Eur. Cell. Mater.* **33**, 158–168 (2017).
29. R. Y. Kwon, S. Temiyasathit, P. Tummala, C. C. Quah, C. R. Jacobs, Primary cilium-dependent mechanosensing is mediated by adenylyl cyclase 6 and cyclic AMP in bone cells. *FASEB J.* **24**, 2859–2868 (2010).
30. M. Delling, P. G. DeCaen, J. F. Doerner, S. Febvay, D. E. Clapham, Primary cilia are specialized calcium signalling organelles. *Nature* **504**, 311–314 (2013).
31. N. Luo, M. D. Conwell, X. Chen, C. I. Kettenhofen, C. J. Westlake, L. B. Cantor, C. D. Wells, R. N. Weinreb, T. W. Corson, D. F. Spandau, K. M. Joos, C. Iomini, A. G. Obukhov, Y. Sun, Primary cilia signaling mediates intraocular pressure sensation. *Pro. Natl. Acad. Sci. U.S.A.* **111**, 12871–12876 (2014).
32. H. A. Praetorius, K. R. Spring, Bending the MDCK cell primary cilium increases intracellular calcium. *J. Membr. Biol.* **184**, 71–79 (2001).
33. S. Su, S. C. Phua, R. DeRose, S. Chiba, K. Narita, P. N. Kalugin, T. Kontani, S. Takeda, T. Inoue, Genetically encoded calcium indicator illuminates calcium dynamics in primary cilia. *Nat. Methods* **10**, 1105–1107 (2013).
34. P. T. Newton, L. Li, B. Zhou, C. Schweingruber, M. Hovorakova, M. Xie, X. Sun, L. Sandhow, A. V. Artemov, E. Ivashkin, S. Suter, V. Dyachuk, M. E. Shahawy, A. Gritli-Linde, T. Bouderlique, J. Petersen, A. Mollbrink, J. Lundeberg, G. Enikolopov, H. Qian, K. Fried, M. Kasper, E. Hedlund, I. Adameyko, L. Sävendahl, A. S. Chagin, A radical switch in clonality reveals a stem cell niche in the epiphyseal growth plate. *Nature* **567**, 234–238 (2019).
35. C. L. Thompson, A. Wiles, C. A. Poole, M. M. Knight, Lithium chloride modulates chondrocyte primary cilia and inhibits Hedgehog signaling. *FASEB J.* **30**, 716–726 (2016).
36. Y.-G. Han, H. J. Kim, A. A. Dlugosz, D. W. Ellison, R. L. Gibertson, A. Alvarez-Buylla, Dual and opposing roles of primary cilia in medulloblastoma development. *Nat. Med.* **15**, 1062–1065 (2009).
37. S. Y. Wong, A. D. Seol, P.-L. So, A. N. Ermilov, C. K. Bichakjian, E. H. Epstein Jr., A. A. Dlugosz, J. F. Reiter, Primary cilia can both mediate and suppress Hedgehog pathway–dependent tumorigenesis. *Nat. Med.* **15**, 1055–1061 (2009).
38. C. L. Thompson, J. P. Chapple, M. M. Knight, Primary cilia disassembly down-regulates mechanosensitive hedgehog signalling: A feedback mechanism controlling ADAMTS-5 expression in chondrocytes. *Osteoarthr. Cartil.* **22**, 490–498 (2014).
39. Y. Y. Shao, L. Wang, J. F. Welter, R. T. Ballock, Primary cilia modulate Ihh signal transduction in response to hydrostatic loading of growth plate chondrocytes. *Bone* **50**, 79–84 (2012).
40. S. C. Phua, S. Chiba, M. Suzuki, E. Su, E. C. Roberson, G. V. Pusapati, M. Setou, R. Rohatgi, J. F. Reiter, K. Ikegami, T. Inoue, Dynamic remodeling of membrane composition drives cell cycle through primary cilia excision. *Cell* **168**, 264–279.e15 (2017).
41. B. Delaval, A. Bright, N. D. Lawson, S. Doxsey, The cilia protein IFT88 is required for spindle orientation in mitosis. *Nat. Cell Biol.* **13**, 461–468 (2011).
42. K. I. Hilgendorf, C. T. Johnson, A. Mezger, S. L. Rice, A. M. Norris, J. Demeter, W. J. Greenleaf, J. F. Reiter, D. Kopinke, P. K. Jackson, Omega-3 fatty acids activate ciliary FFAR4 to control adipogenesis. *Cell* **179**, 1289–1305.e21 (2019).
43. D. Kopinke, E. C. Roberson, J. F. Reiter, Ciliary Hedgehog signaling restricts injury-induced adipogenesis. *Cell* **170**, 340–351.e12 (2017).
44. F. Fang, S. P. Lake, Multiscale strain analysis of tendon subjected to shear and compression demonstrates strain attenuation, fiber sliding, and reorganization. *J. Orthop. Res.* **33**, 1704–1712 (2015).
45. F. Fang, S. P. Lake, Experimental evaluation of multiscale tendon mechanics. *J. Orthop. Res.* **35**, 1353–1365 (2017).
46. S. T. Christensen, S. K. Morthorst, J. B. Mogensen, L. B. Pedersen, Primary cilia and coordination of receptor tyrosine kinase (RTK) and transforming growth factor β (TGF-β) signaling. *Cold Spring Harb. Perspect. Biol.* **9**, a028167 (2017).
47. E. Blitz, S. Viukov, A. Sharir, Y. Shwartz, J. L. Galloway, B. A. Pryce, R. L. Johnson, C. J. Tabin, R. Schweitzer, E. Zelzer, Bone ridge patterning during musculoskeletal assembly is mediated through SCX regulation of *Bmp4* at the tendon-skeleton junction. *Dev. Cell* **17**, 861–873 (2009).
48. J. W. Maricelli, Q. L. Lu, D. C. Lin, B. D. Rodgers, Trendelenburg-like gait, instability and altered step patterns in a mouse model for limb girdle muscular dystrophy 2i. *PLOS ONE* **11**, e0161984 (2016).
49. I. Kurtaliaj, M. Golman, A. C. Abraham, S. Thomopoulos, Biomechanical Testing of Murine Tendons. *J. Vis. Exp.*, e60280 (2019).

Acknowledgment: We thank M. Yang from the Mouse Neurobehavior Core at Columbia University for facilitating mouse gait analysis experiments. **Funding:** The study was funded by NIH R01 AR055580. Confocal imaging was performed in the Confocal and Specialized Microscopy Shared Resource of the Herbert Irving Comprehensive Cancer Center at Columbia University, supported by an NIH grant P30 CA013696 (National Cancer Institute).
Author contributions: F.F. developed the hypotheses and study design, performed

experiments, analyzed data, drafted, and edited the manuscript. A.G.S. performed experiments and edited the manuscript. E.R.M. developed methods and edited the manuscript. M.E.S. performed experiments and edited the manuscript. S.T. conceived the study, developed hypotheses and study design, analyzed data, drafted, and edited the manuscript. **Competing interests:** The authors declare that they have no competing interests. **Data and materials availability:** All data needed to evaluate the conclusions in the paper are present in the paper and/or the Supplementary Materials. Additional data related to this paper may be requested from the authors.

Submitted 10 April 2020
Accepted 17 September 2020
Published 30 October 2020
10.1126/sciadv.abc1799

Citation: F. Fang, A. G. Schwartz, E. R. Moore, M. E. Sup, S. Thomopoulos, Primary cilia as the nexus of biophysical and hedgehog signaling at the tendon enthesis. *Sci. Adv.* **6**, eabc1799 (2020).